Polymer Bulletin 32, 193–200 (1994)

Polymer Bulletin

Effect of thermal molecular motion on pervaporation behavior of comb-shaped polymers with fluorocarbon side groups

V. V. Volkov[1], A. G. Fadeev[1], N. A. Plate[1], N. Amaya[2], Y. Murata[2], A. Takahara[3], and T. Kajiyama[3,*]

[1]A. V. Topchiev Institute of Petrochemical Synthesis, Russian Academy of Sciences, Leninsky Prospect, 29, 117912 GSP-1 Moscow B-71, Russia
[2]Tsukuba Research Laboratory, Nippon Oil and Fats, Co., Ltd., Tokodai 5-10, Tsukuba, Ibaraki 300-26, Japan
[3]Department of Chemical Science and Technology, Faculty of Engineering, Kyushu University, Higashi-ku, Fukuoka 812, Japan

Summary

Thermal molecular motion of a series of comb-shaped polymers with heptadecafluorodecyl side chains ($C^F_8C_2$-) has been studied based on dynamic viscoelastic measurement. The main chain of comb-shaped polymers was poly(fumarate), poly(methacrylate), and poly(acrylate). Poly(fluoroalkylfumarate) with heptadecafluorodecyl group, P($C^F_8C_2$-iPF) was amorphous polymer, whereas poly(acrylate) and poly(methacrylate) with $C^F_8C_2$-, P($C^F_8C_2$-Acr) and P($C^F_8C_2$-MAcr) showed mesomorphic behavior. The pervaporation behavior of water/organic mixtures through amorphous polymer, P($C^F_8C_2$-iPF), and mesomorphic one, P($C^F_8C_2$-Acr), were investigated. The distinct increase in permselectivity has been observed at the mesomorphic transition of P($C^F_8C_2$-Acr).

Introduction

The comb-shaped polymers having fluorocarbon segments in their side chain part have attracted a particular attention due to the very low values of surface free energy [1-5]. Recently, aggregation states were investigated for a series of comb-shaped polymers such as poly(acrylate), poly(methacrylate) and disubstituted poly(fumarates) containing fluoroalkyl group in the side chain part, on the basis of differential scanning calorimetry (DSC) and wide-angle X-ray diffraction (WAXD) measurements and polarizing optical microscopic (POM) observation in a wide temperature range [1,6]. All poly(fluoroalkylfumarates) were amorphous polymers, but poly(fluoroalkylmethacrylate) and poly(fluoroalkylacrylate) having heptadecafluorodecyl ($C^F_8C_2$-) group in the side chain part (P($C^F_8C_2$-Acr) and P($C^F_8C_2$-MAcr), respectively) were in a mesomorphic state at room temperature [1,6]. The type of mesophase was identified as ordered smectic liquid crystalline (LC) structure of smectic B modification (S_B) for P($C^F_8C_2$-Acr) and an unordered smectic LC structure of smectic A modification (S_A) for P($C^F_8C_2$-MAcr). The mesogenic phase in these cases was induced by perfluoroalkyl C_8F_{17} groups. The pronounced transitions were observed from smectic to isotropic phase at 350 K for P($C^F_8C_2$-Acr) and 360 K for P($C^F_8C_2$-MAcr).

In this study, the dynamic viscoelastic measurement was carried out in order to reveal the thermal molecular motions in comb-shaped polymers such as poly(acrylate), poly(methacrylate) and disubstituted poly(fumarates) containing heptadecafluorodecyl group in the side chain part. Also, pervaporation behaviors of water/organic mixtures through the P($C^F_8C_2$-iPF) and P($C^F_8C_2$-Acr) membranes were investigated in a temperature range including their phase transition region.

*Corresponding author

Experimental

Materials

Poly(fluoroalkylfumarates) (PFAF), poly(fluoroalkylacrylate) (PFAA), poly(fluoroalkylmethacrylate) (PFAMA) were prepared by a radical polymerization. Polymerization procedure was similar to that for poly(alkylfumarate) (PAF) [7]. Figure 1 shows the chemical structures of poly(3,3,4,4,5,5,6,6,7,7,8,8,9,9,10,10,10-heptadecafluorodecyl isopropyl fumarate) ($P(C_8^FC_2$-iPF)), poly(3,3,4,4,5,5,6,6,7,7,8,8,9,9,10,10,10-heptadecafluorodecyl methacrylate ($P(C_8^FC_2$-MAcr)) and poly(3,3,4,4,5,5,6,6,7,7,8,8,9,9,10,10,10-heptadecafluorodecyl acrylate) ($P(C_8^FC_2$-Acr)). Polymer films for physicochemical and pervaporation investigations were prepared by casting each polymer solution on a clean glass plate or cellophane support, air-dried at room temperature for 24 hours and then, dried in vacuo until the constant weight was attained. The solvent used was 1,1,2-trifluorotrichloroethane.

Dynamic Viscoelastic Measurement

The temperature dependences of the dynamic viscoelasticity were measured by dynamic spring analysis [8] by dynamic with Rheovibron DDVII-C (Orientec Co., Ltd.) at the frequency of 3.5, 11 and 110Hz under a dried nitrogen purge. A spiral spring of ca. 2mm in diameter was made of copper wire. Polymer thin film was cast by coating a polymer solution on the spring surface and dried in vacuo.

Pervaporation Experiment

Figure 2 shows a diagram of the pervaporation testing system used in this study. The films were installed into a pervaporation cell on a porous metallic support and sealed by using a flat rubber gasket. Effective membrane area was 19.6 cm^2. Pervaporation of water/ethanol and water/acetone mixtures was investigated in a temperature range from 288 to 363K. During the experiment, the feed mixture was supplied to the center of the cell through the tube which locates 0.5cm away from membrane surface and removed through the outlet in the upper compartment of the cell. A circulation of feed

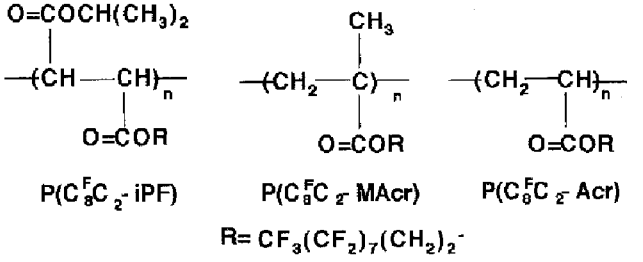

Figure 1 Chemical structures of poly(fumarate), poly(fluoroalkylmethacrylate), and poly(fluoroalkylacrylate) with heptadecafluorodecyl side chain.

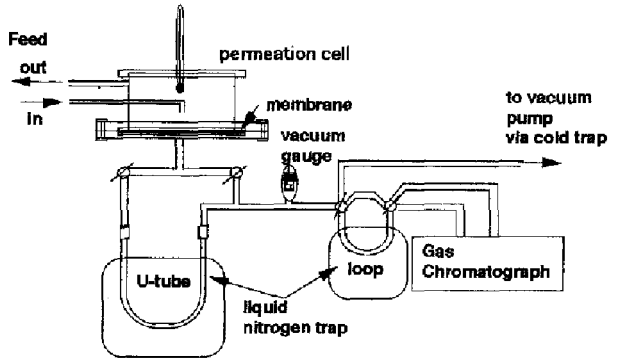

Figure 2. Schematic representation of the pervaporation apparatus.

mixture (0.5-0.7 dm^3 min^{-1}) and temperature control (+0.2K) were achieved by using a liquid thermostat. In the course of experiments, the composition of feed mixture was measured chromatographically and maintained constant by adding a more volatile component. The lower compartment of the cell was evacuated with a vacuum pump. Operating pressure of this experiment was about 2mmHg. Depending on the total flux, two different permeate analysis techniques were used. At low fluxes, the permeate was accumulated in a liquid nitrogen-cooled loop. After some time, the loop was disconnected from the cell by using a cock and heated to a room temperature. As a result, all the collected permeate passed into vapor phase. The permeation in vapor phase was carried by He carrier gas from a loop to a gas chromatograph for analysis. If freezing time was less than 10 sec due to greater permeate flux in a higher temperature range, another technique was used. In this case, the permeate was accumulated in a removable U-shaped tube cooled by liquid nitrogen. Weighing the U-shaped tube containing liquid permeate on analytical balance was used to determine total flux, whereas the composition of permeate mixture was analyzed refractometrically and chromatographically by injecting a liquid permeate into gas chromatograph with a microsyringe. Thus, the validity of the results has been confirmed by two different methods.

Results and Discussion

Viscoelastic Properties

Figure 3 shows the temperature dependences of tanδ for P($C_8F$$C_2$-iPF), P($C_8F$$C_2$-MAcr), and P($C_8F$$C_2$-Acr) at 11Hz. The large absorptions were observed at 360, 380 and 365K for P($C_8F$$C_2$-IPF), P($C_8F$$C_2$-MAcr), and P($C_8F$$C_2$-Acr), respectively. Also, a shoulder was observed at 330K for P($C_8F$$C_2$-iPF). The width of the peaks decreased in the following order: P($C_8F$$C_2$-iPF), P($C_8F$$C_2$-MAcr), and P($C_8F$$C_2$-Acr). The magnitude of activation energies for these main peaks were equal to 164, 430, and 1860 kJ mol^{-1} for P($C_8F$$C_2$-iPF), P($C_8F$$C_2$-MAcr), and P($C_8F$$C_2$-Acr), respectively. In our previous report, DSC measurement, polarizing optical microscopic and wide angle X-ray diffraction measurement of these comb-shaped polymers revealed that P($C_8F$$C_2$-MAcr) and P($C_8F$$C_2$-Acr) can form mesomorphic phase. The width of the peak and the value of the activation energy reflect the

degree of ordering of polymers under consideration, namely, amorphous state, unordered smectic (S_A) and ordered smectic (S_B) states for P($C_8^FC_2$-iPF), P($C_8^FC_2$-MAcr), and P($C_8^FC_2$-Acr), respectively.

The nature of the molecular mobility in comb-shaped polymers is strongly dependent on the presence of long side chains and the possibility of internal rotation of the atoms in the main and side chains. The different type of motion very often takes place simultaneously in a similar region of frequency or temperature that impedes their assignments and unambiguous interpretation for thermal molecular motions. Nevertheless, some speculations can be done on the basis of the results obtained. It is apparent from the CPK (Coury-Pauling-Kolton) molecular models that PFAF studied here consist of a rigid backbone chain. The repulsive force between neighboring ester groups is a reason of high main chain rigidity. Therefore, it is reasonably assumed that the large tanδ absorptions observed at ca.360K for P($C_8^FC_2$-iPF), is associated with the side isopropyl ester motion (β_{iP}). It should be noted that the absorption at around 400K was observed for all disubstituted poly(fumarates) containing isopropyl groups. Those were including poly(diisopropyl fumarate) (P(diPF)) [9], poly(sec-butyl isopropylfumarates) (P(sB-iPF)), poly(4-methylpentyl isopropylfumarate) (P(4m-iPF)), and poly(cyclohexyl isopropylfumatrate) (P(cH-iPF)) [10]. The mean activation energy of 164kJ mol^{-1} obtained in this study for P($C_8^FC_2$-iPF) is not contradictory to the aforementioned assumption. Michailov and Borisova reported that the magnitude activation energy for the β process in poly(isopropyl methacrylate) (PIPMA) was 67kJ mol^{-1} [11]. This process arises from the hindered rotation of the isopropyl group around the C-C bond that links it to the main chain. On the other hand, the activation energy of 215kJ mol^{-1} for the β-absorption (β_{iP}) at around 400K was reported for P(diPF) [9]. It was concluded that in the case of P(diPF), the rotation of ester groups would be highly hindered compared with that in PIPMA due to a presence of a more bulky side group of diPF and then, give rise to an increased value of activation energy.

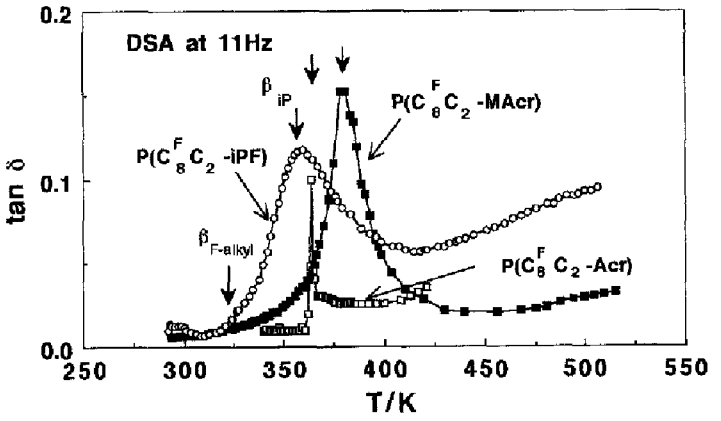

Figure 3. Temperature dependence of tanδ for P($C_8^FC_2$-iPF), P($C_8^FC_2$-MAcr), and P($C_8^FC_2$-Acr) under dynamic spring analysis (DSA) at 11Hz.

Based on POM, DSC and WAXD studies of uniaxially drawn films of P($C_8^FC_2$-iPF), it was reported that there were two temperature regions is in the vicinity of 325K and 360K, in which distinct change in the thermal molecular motion took place [6]. It can be speculated that the first relaxation process at ca.325K could be assigned to the softening of long side groups of P($C_8^FC_2$-iPF) and the second one at ca.360K is associated with rotational motion of isopropyl groups. The cross section of the spacer fragment (two methylene unit) in the side fluorocarbon group of P($C_8^FC_2$-iPF) is less than that for isopropyl group. Therefore, the rotational mobility of isopropyl group in P($C_8^FC_2$-iPF) is less hindered than that in P(diPF) but much more hindered than that in PiPMA. As a result, the activation energy for P($C_8^FC_2$-iPF) has a value (164 kJ mol^{-1}) between these for PiPMA (67 kJ mol^{-1}) and P(diPF) (215 kJ mol^{-1}) as mentioned above. As has been suggested for the case of P(diPF) [9], it is assumed that aforementioned side chain motion does not result in a large decrease of the rigidity of the backbone chain for all comb-shaped poly(fumarates) considered in this work. The main chain motion as a whole is restricted by the ester groups and micro-Brownian motion of the backbone chains does not seemingly occur until the decomposition of the polymers at high temperature.

Pervaporation Behavior

Pervaporation of water/organic mixtures through the P($C_8^FC_2$-iPF) and P($C_8^FC_2$-Acr) films was examined in order to reveal the interrelation among aggregation state, thermal molecular motion, and permselectivity of comb-shaped polymers. As expected from their chemical structures, both polymers featured preferential permeation of organic component compared to water.

Pervaporation of ethanol/water mixture with the ethanol content of 4wt% through the P($C_8^FC_2$-iPF) film was investigated in the temperature range of 288-363K. Figure 4 shows the Arrehenius plot of flux of the ethanol/water mixture permeation rate for the P($C_8^FC_2$-iPF) film. The experimental data followed linear dependence. Table 1 shows the magnitudes of apparent activation energies for ethanol and water pervaporation through the P($C_8^FC_2$-iPF) film. Figure 5 shows the temperature dependence of separation factor for P($C_8^FC_2$-iPF) film. The separation factor (selectivity) was calculated by using following equation,

$$\alpha=(C'_O/C'_W)/(C_O/C_W)$$

where C_O, C'_O, C_W, and C'_W are organic component concentration in feed mixture and permeate

Table 1 Magnitude of activation energy for pervaporation of ethanol and water mixture through P($C_8^FC_2$-iPF)

Permeant	Activation energy/kJ mol^{-1}	
	Refractometer	Chromatograph
Ethanol	59.9 ± 1.6	57.5 ± 0.8
Water	47.6 ± 0.4	45.1 ± 0.8

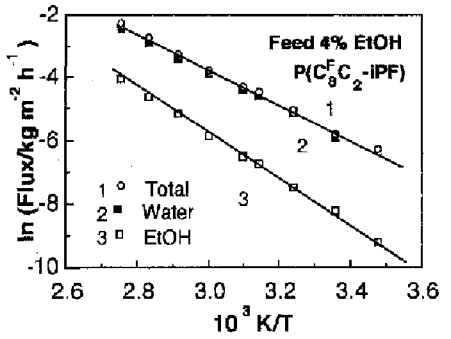

Figure 4. Arrehenius plot of flux of ethanol/ water mixture through P($C_8^FC_2$-iPF) .

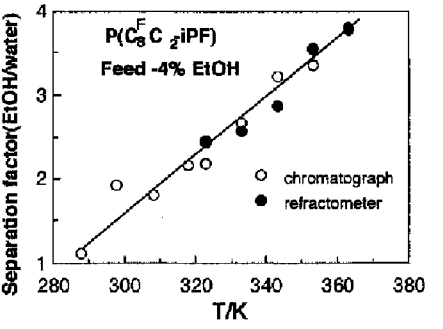

Figure 5. Temperature dependence of separation factor of ethanol/water mixture through P($C_8^FC_2$-iPF) .

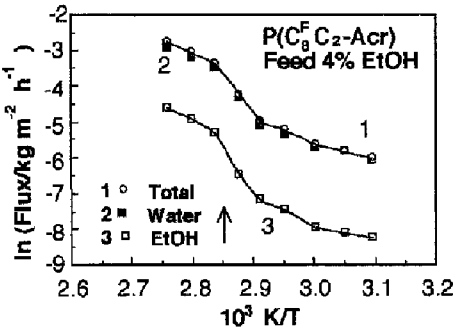

Figure 6. Arrehenius plot of flux of ethanol/ water mixture through P($C_8^FC_2$-Acr) .

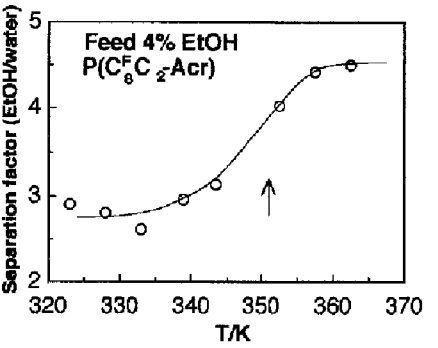

Figure 7. Temperature dependence of separation factor of ethanol/water mixture through P($C_8^FC_2$-Acr) .

and water component concentration in feed mixture and permeate, respectively. It is apparent from Figure 5 and Table 1 that the results obtained by using refractometry and gas chromatography are in good agreement. The separation factor and permeation rate through the P($C_8^FC_2$-iPF) film increased linearly with temperature, which corresponded to the increase in mechanical tanδ at this temperature region.

Completely different behavior was observed for mesomorphic polymer, P($C_8^FC_2$-Acr). Figure 6 shows the Arrehenius plot of flux of ethanol/water mixtures through the P($C_8^FC_2$-Acr) film. The reciprocal temperature dependence of flux for the P($C_8^FC_2$-Acr) film was sigmoidal shape and could be divided into three different regions, that is, below 343K, between 343 and 353K, and above 353K. Below 343K, the flux increased slightly with temperature. In the temperature range between 343-353K, a significant increase in permeability was observed. Figure 7 shows the temperature dependence of the separation factor for ethanol/water mixture through the P($C_8^FC_2$-Acr) film. The separation factor also featured sigmoidal shape and its inflection point was observed also at around 343-353K. The temperature range, at which the flux and separation factor started to increase was slightly lower than the mesomorphic-isotropic phase transition temperature of P($C_8^FC_2$-Acr) [6]. This might be ascribed to plasticizing effect by the presence of permeant in the film.

A significantly pronounced effect was observed for pervaporation of acetone/water mixture through the P($C_8^FC_2$-Acr) film. Figure 8 shows the Arrehenius plot of flux of acetone/water mixtures through the P($C_8^FC_2$-Acr) film. The concentration of acetone in feed solution was 4%. The temperature dependence of flux for the P($C_8^FC_2$-Acr) film also showed sigmoidal shape and its change was more distinct compared with that obtained for pervaporation of ethanol/water. The flux increased a factor of more than 10 in the temperature range studied here. Figure 9 shows the temperature dependence of the separation factor for acetone/water mixture through the P($C_8^FC_2$-Acr) film. In this case, acetone/water separation factor featured more pronounced S-shaped character with an abrupt jump to 32-34, approaching to the phase transition point of 350K. Similar behavior has been observed for the gas permeation or ion permeation through the (polymer/liquid crystal) composite system [12-14] and the polymer/(artificial amphiphile) composite system [15,16] at their crystal-liquid crystal phase transition temperature.

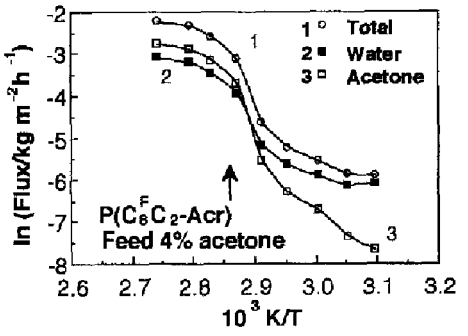

Figure 8. Arrehenius plot of flux of acetone/water mixture through P($C_8^FC_2$-Acr).

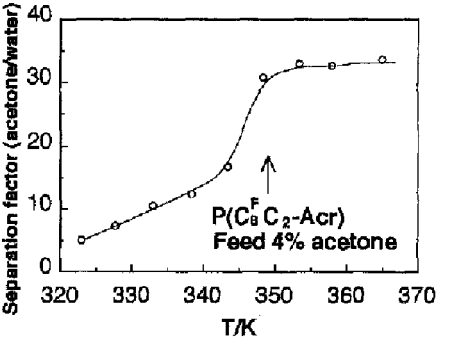

Figure 9. Temperature dependence of separation factor of acetone/water mixture through P($C_8^FC_2$-Acr).

Acknowledgement

Dr. V. V. Volkov acknowledge support provided by the Japan Society for the Promotion of Science (JSPS) during his half a year staying at the Department of Chemical Science & Technology, Kyushu University, Fukuoka, Japan.

References

1 Takahara A, Choi SB, Amaya N, Murata Y, Kajiyama T (1987) Rept Progr Polym Phys Japan 30:187
2 Ramharack R, Nguyen TH (1987) J Polym Sci Polym Lett 25:93
3 Pittman AG, Ludwig B A(1969) J Polym Sci A1-7: 3053
4 Pittman AG, Sharp DL, Ludwig BA(1969) J Polym Sci A1-6: 1729
5 Bernett MK, Zisman WA (1962) J Phys Chem 66:1207,
6 Volkov VV, Plate NA, Takahara A, Amaya N, Murata Y, Kajiyama T (1992) Polymer 31:1316
7 Otsu T, Ito O, Toyoda N, Mori S (1981) Makromol Chem Rapid Commun 2:725.
8 Naganuma S, Sakurai T, Takahashi Y, Takahashi S (1972) Kobunshi Ronbunshu 105:519
9 Yamada K, Takayanagi M, Murata Y (1986) Polymer 27:1054
10 Choi SB, Takahara A, Amaya N, Murata Y, Kajiyama T (1989) Polym. J. 21:215
11 Michailov GP, Borisova TI (1985) Soc Phys Tech Phys 3: 120
12 Kajiyama T, Nagata Y, Maemura E, Takayanagi M (1979) Chem Lett:679,
13 Kajiyama T, Nagata Y, Washizu S, Takayanagi M (1982) J Membrane Sic 11:39
14 Kajiyama T, Washizu S, Takayanagi M (1984) J Appl Polym Sci 29:3955
15 Kajiyama T, Kumano A, Takayanagi M, Okahata Y, Kunitake T (1979) Chem Lett:645
16 Kajiyama T, Kumano A, Takayanagi M (1984) In Contemporary Topics in Polymer Science, Vol.4, (W. J. Bailey and T. Tsuruta Eds)., Plenum Pub, New York, p.829

Accepted December 9, 1993 S